ISME

R. Bagheri[*]
Ph.D Student

M. Ayatollahi[†]
Associate Professor

O. Rahmani[‡]
Assistant Professor

Multiple Moving Cracks in a Non-homogeneous Orthotropic Strip

The problem of several finite moving cracks in a functionally graded material is solved by dislocation technique under the condition of anti-plane deformation. By using the Fourier transform the stress fields are obtained for a functionally graded strip containing a screw dislocation. The stress components reveal the familiar Cauchy singularity at the location of dislocation. The solution is employed to derive integral equations for a strip weakened by several moving cracks. Numerical examples are provided to show the effects of material properties, the crack length and the speed of the crack propagating upon the stress intensity factor and strain energy density factor.

Keywords: Crack propagation, Non-homogeneous orthotropic material, Dynamic stress intensity factor, Strain energy density factor

1 Introduction

In recent years, the functionally graded materials have widely been introduced and applied in the environments with extremely high temperature. The study of dynamic fracture mechanics of non-homogeneous orthotropic materials is therefore an active research area. In many engineering applications, non-homogeneous structures may be subjected to dynamic behaviors. The dynamic manipulation of such structures may lead to crack formation and eventually the failures of the structures. The knowledge of crack propagation in non-homogeneous orthotropic material is important in designing components of FGMs and improving their fracture toughness. Problems of crack propagation at constant speed can be classified into three classes depending on the boundary conditions [1]. The first class is the steady-state crack growth. Here, the crack tip moves at constant speed for all the time and the mechanical fields are invariant with respect to an observer moving with the crack tip. The prototype problem in this category is the two-dimensional Yoffe problem of a crack of fixed length propagating in a body subjected to uniform far field tensile loading, [2]. The second class of problems is the self-similar crack growth subject to time-independent loading. In this case, the crack tip has been moving at constant speed since some initial instant, and certain mechanical fields are invariant with respect to an observer moving steadily away from the

[*] Ph.D Student ,Faculty of Engineering, University of Zanjan, rasul_m65@yahoo.com
[†] Corresponding Author, Associate Professor, Mechanical Engineering, University of Zanjan, mo_ayatollahy@yahoo.com
[‡] Assistant Professor, Mechanical Engineering, University of Zanjan, Omid.Rahmani@znu.ac.ir

process being observed. The third category of problems corresponds to crack in a body initially at rest and subjected to time-independent loading. There has been significant progress in the study of fracture behavior of FGMs is considered mainly on static cases. There is a yet a lack of dynamic fracture mechanics study of FGMs due to the complexity in solution. Sih and Chen. [3] studied the dynamic behavior of a moving crack in layered composites. Wang and Meguid [4] introduced a theoretical and numerical treatment of a finite crack propagating in an interfacial layer with spatially varying elastic properties under the anti-plane loading. The dynamic crack propagation in FGMs under the plane elastic deformation using Fourier transform technique was investigated by Meguid et al [5]. Jiang and Wang [6] studied the dynamic behavior of a Yoffe type crack propagating in a functionally graded interlayer bonded to dissimilar half planes. The dynamic stress intensity factor and strain energy density for moving crack in an infinite strip of functionally graded material subjected to antiplane shear was determined by Bi et al. [7]. Li [8] solved the dynamic problem of an impermeable crack of finite length propagating in a piezoelectric strip. The dynamic propagating of anti-plane shear cracks in functionally graded piezoelectric strip was investigated by Kwon [9]. A finite crack with constant length propagating in the functionally graded orthotropic strip under in plane loading was investigated by Ma et al. [10]. The effects of material properties, the thickness of the functionally graded orthotropic strip and the speed of the crack propagating upon the dynamic fracture behavior were studied. Das [11], investigated the interaction between three moving collinear Griffith cracks under antiplane shear stress situated at the interface of an elastic layer overlying a different half plane. The problem of a Griffith crack of constant length propagating at a uniform speed in a non-homogeneous plane under uniform load was studied by Singh et al. [12]. Wang and Han [13], considered the problem of a moving crack in a non-homogeneous material strip. They found that the maximum anti-plane shear stress around the crack tip is a suitable failure criterion for moving cracks. In the next work, Wang and Han investigated the dynamic behavior of a crack moving at the interface between an FGM layer and homogeneous substrate [14]. The finite crack with constant length (Yoffe-type crack) propagating in a functionally graded strip with spatially varying elastic properties between two dissimilar homogeneous layers under in-plane loading was studied by Cheng and Zhong. [15]. The solution procedures devised in all above studies are neither capable of handling multiple cracks nor arbitrary arrangement. Bagheri and Ayatollahi [16] investigated the problem of several finite cracks with constant length propagating in a functionally graded strip. The effects of the geometric parameters, the crack length, and the speed of the propagating cracks upon the stress intensity factors were investigated.

The objective of the present study is to provide a theoretical analysis of the dynamic fracture behavior of a Yoffe type crack propagating in a non-homogeneous orthotropic strip. The elastic stiffness constants and mass density of materials are assumed to vary exponentially perpendicular to the direction of the crack propagation. This paper presents a procedure to analyze the dynamic stress intensity factors and strain energy density factors of multiple moving cracks with arbitrarily patterns located at the functionally graded orthotropic strip. The Galilean transformation is employed to express the wave equations in terms of coordinates that are attached to the moving crack. To confirm the validity of formulations, numerical values of dynamic stress intensity factors for a crack is compared with the results in literature. Numerical results are given for the different shear moduli gradient, moving crack speed, non-homogeneous coefficient, and ratios of shear moduli.

2 Methodology and formulation

A non-homogeneous orthotropic strip with thickness h is shown in figure (1).

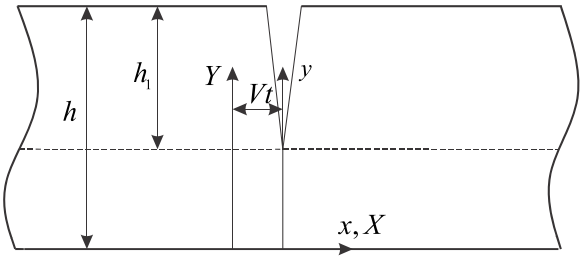

Figure 1 Schematic view of a functionally graded orthotropic strip with a screw dislocation

The distributed dislocation technique is an efficient means for treating multiple moving cracks with smooth geometry. However, determining stress fields due to a single dislocation in the region has been a major obstacle to the utilization of this method. We now take up this task for an orthotropic functionally graded strip containing a moving screw dislocation. The basic equations which govern the anti-plane deformation of the orthotropic functionally graded strip can be expressed in a Cartesian coordinate system as :

$$\begin{aligned} &\frac{\partial \sigma_{zx}}{\partial X}+\frac{\partial \sigma_{zy}}{\partial Y}=\rho(Y)\frac{\partial^2 W}{\partial t^2} \\ &\sigma_{zx}(X,Y,t)=\mu_x(Y)\frac{\partial W}{\partial X} \\ &\sigma_{zy}(X,Y,t)=\mu_y(Y)\frac{\partial W}{\partial Y} \end{aligned} \tag{1}$$

Where W is the component of displacement in the $z-$direction and $\mu_x(Y),\mu_y(Y)$ are the shear modulus of the material. Dynamic anti-plane governing equations of motion for non-homogeneous orthotropic materials can be expressed by displacement component as:

$$\frac{\partial^2 W}{\partial X^2}+\frac{2\lambda}{f^2}\frac{\partial W}{\partial Y}+\frac{1}{f^2}\frac{\partial^2 W}{\partial Y^2}=\frac{1}{C_x^2}\frac{\partial^2 W}{\partial t^2} \tag{2}$$

Where $\rho(Y)$ is the material mass density, It should be noted that body forces are not considered in the present work. In order to over come the complexity of the mathematics involved, we shall focus in this study on a special class of non-homogeneous materials in which the property variations are in the same proportion and have exponential forms which equilibrium has an analytical solution. Therefore, we assume

$$\begin{aligned} &[\mu_x(Y),\mu_y(Y),\rho(Y)]=[\mu_{0x}\mu_{0y},\rho_0]e^{2\lambda Y} \\ &C_x=\sqrt{\mu_{0x}/f}\,,\ f=\sqrt{\mu_{0x}/\mu_{0y}} \end{aligned} \tag{3}$$

Where μ_{0y},μ_{0x},ρ_0 and λ are material constants. In order to simplify Eq. (2), the Galilean transformation is taken

$$X=x+Vt,\quad Y=y,\quad \frac{\partial}{\partial t}=V\frac{\partial}{\partial x}. \tag{4}$$

Substituting Eq. (3) and (4) into Eq. (2) results in the following governing equations for the non-homogeneous orthotropic strip

$$f^2(1-V^2/C_x^2)\frac{\partial^2 w}{\partial x^2}+\frac{\partial^2 w}{\partial y^2}+2\lambda\frac{\partial w}{\partial y}=0 \tag{5}$$

For the dislocation solution, since no traction is applied on both the upper and the lower boundary, the following conditions on the strip boundaries must be satisfied

$$\sigma_{zy}(x,0)=0,\sigma_{zy}(x,h)=0 \tag{6}$$

For the strip depicted in figure (1), the continuity and limiting conditions may be expressed

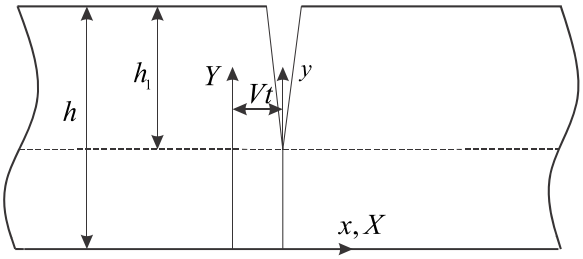

Figure 1 Schematic view of a functionally graded orthotropic strip with a screw dislocation

$$\begin{aligned} &w(0^+,y)-w(0^-,y)=b_z H(y-h_1)\\ &\sigma_{zy}(x,h_1^+)=\sigma_{zy}(x,h_1^-)\\ &\lim_{|x|\to\infty} w=0 \end{aligned} \tag{7}$$

Here, $H(y)$ is the Heaviside step-function. The first Eq. (7) shows the multi valuedness of displacement while the second implies the continuity of traction along the dislocation line. It is worth mentioning that the above conditions for screw dislocation were utilized by several investigators, e. g., Weertman and Weertman [17]. Equation (5) is solved by means of the Sine Fourier transform. The Fourier sine transform is defined as

$$F(\zeta)=\int_0^{+\infty}\sin(\zeta x)\,f(x)dx \tag{8}$$

The inversion of (8) yields:

$$f(x)=\frac{2}{\pi}\int_0^{+\infty}\sin(\zeta x)F(\zeta)d\zeta \tag{9}$$

The solution to Eq. (5) in the two regions $0<y<h-h_1$ and $h-h_1<y<h$ is achieved by means of the Fourier sine transform to eliminate the x variable yielding a second order ordinary differential equation for $w^*(\zeta,y)$. Following a routine methodology the transformed displacement field in the whole region reduces to

$$\begin{aligned} w^*(\zeta,y)=&-\frac{b_z\sinh(\beta h_1)e^{\lambda(h_1-y)}}{4\beta\zeta\sinh(\beta h)}\{(\beta+\lambda)e^{-\beta h}e^{y\sqrt{\lambda^2+\zeta^2 f^2(1-V^2/C_x^2)}}\\ &-(\beta-\lambda)e^{\beta h}e^{-y\sqrt{\lambda^2+\zeta^2 f^2(1-V^2/C_x^2)}}\}+\frac{b_z}{2\zeta} \qquad h_1\le y\le h\\ w^*(\zeta,y)=&-\frac{b_z\sinh(\beta(h_1-h))e^{\lambda(h_1-y)}}{4\beta\zeta\sinh(\beta h)}\{(\beta+\lambda)e^{y\sqrt{\lambda^2+\zeta^2 f^2(1-V^2/C_x^2)}}\\ &-(\beta-\lambda)e^{-y\sqrt{\lambda^2+\zeta^2 f^2(1-V^2/C_x^2)}}\} \qquad 0\le y\le h_1 \end{aligned} \tag{10}$$

Where $\beta=\sqrt{\lambda^2+\zeta^2 f^2(1-V^2/C_x^2)}$. The displacement component in view of (9) and (10) leads to:

$$w(x,y)=-\frac{b_z e^{-\lambda(y-h_1)}}{\pi}\int_0^{\infty}\frac{\sinh(\beta h_1)}{\beta\zeta\sinh(\beta h)}[\beta\cosh(\beta(h-y))-\lambda\sinh(\beta(h-y))]\sin(\zeta x)d\zeta$$
$$+\operatorname{sgn}(x)b_z \qquad h_1\le y\le h$$
$$w(x,y)=-\frac{b_z e^{-\lambda(y-h_1)}}{\pi} \qquad (11)$$
$$\times\int_0^{\infty}\frac{\sinh(\beta(h_1-h))}{\beta\zeta\sinh(\beta h)}[\beta\cosh(\beta y)+\lambda\sinh(\beta y)]\sin(\zeta x)d\zeta \qquad 0\le y\le h_1$$

It is elementary to show that Eqs. (11) satisfy the first condition (7). The stress components by virtue of Eqs. (1) and (11), are expressed as :

$$\sigma_{zy}(x,y)=\frac{\mu_{0y}b_z f^2(1-V^2/C_x^{\,2})e^{\lambda(y+h_1)}}{\pi}$$
$$\times\int_0^{+\infty}\frac{\zeta\sinh(\beta h_1)}{\beta\sinh(\beta h)}\sinh(\beta(y-h))\sin(\zeta x)d\zeta \qquad h_1\le y\le h$$
$$\sigma_{zy}(x,y)=\frac{\mu_{0y}b_z f^2(1-V^2/C_x^{\,2})e^{\lambda(y+h_1)}}{\pi} \qquad (12)$$
$$\times\int_0^{+\infty}\frac{\zeta\sinh(\beta(h-h_1))}{\beta\sinh(\beta h)}\sinh(\beta y)\sin(\zeta x)d\zeta \qquad 0\le y\le h_1$$

The stress fields (12) are singular at the location of dislocation. To examine the singular behavior asymptotic analysis of integral as $\zeta\to\infty$, is carried out leading to the following expressions for stress components.

$$\sigma_{zy}(x,y)=\frac{\mu_{0y}b_z e^{\lambda(y+h_1)}f\sqrt{(1-V^2/C_x^{\,2})}}{\pi}$$
$$\times\{\int_0^{\infty}(\frac{f\sqrt{(1-V^2/C_x^{\,2})}\,\zeta\sinh(\beta h_1)}{\beta\sinh(\beta h)}\sinh(\beta(y-h))+e^{-\zeta f\sqrt{(1-V^2/C_x^{\,2})}(y-h_1)})\sin(\zeta x)d\zeta$$
$$-\frac{x}{x^2+f^2(1-V^2/C_x^{\,2})(y-h_1)^2}\} \qquad h_1\le y\le h$$

$$\sigma_{zy}(x,y)=\frac{\mu_{0y}b_z e^{\lambda(y+h_1)}f\sqrt{(1-V^2/C_x^{\,2})}}{\pi}$$
$$\times\{\int_0^{\infty}(\frac{f\sqrt{(1-V^2/C_x^{\,2})}\,\zeta\sinh(\beta(h-h_1))}{\beta\sinh(\beta h)}\sinh(\beta y)-e^{\zeta f\sqrt{(1-V^2/C_x^{\,2})}(y-h_1)})\sin(\zeta x)d\zeta$$
$$+\frac{x}{x^2+f^2(1-V^2/C_x^{\,2})(y-h_1)^2}\} \qquad 0\le y\le h_1$$
(13)

All integrals in Eq. (13) decay reasonably fast as $|\zeta|\to\infty$. Consequently, integrals are regular and stress fields exhibit the familiar Cauchy type singularity at dislocation location.

Alternatively, the contour integration is utilized to evaluate integrals in Eqs. (12). Choosing the proper contours of integration, the final results are

$$\sigma_{zy}(x,y) = -\frac{\mathrm{sgn}(x)\mu_{0y} b_z e^{\lambda(y+h_1)}}{2h} \times \sum_{n=1}^{\infty}[\cos(\frac{n\pi}{h}(h_1-y)) - \cos(\frac{n\pi}{h}(h_1+y))]e^{\frac{-|x|}{f\sqrt{(1-V^2/C_x^2)}}\sqrt{(\frac{n\pi}{h})^2+\lambda^2}} \tag{14}$$

Where $\mathrm{sgn}(x)$ is the sign function. For the sake of brevity, the details of manipulation are not given here. For small values of $|x|$ the series solutions (14) converge slowly and a large number of terms are required to obtain accurate results. To circumvent this difficultly the integrations in (13) should be performed differently. It is easy to show that stress fields, decay exponentially as $n \to \infty$.

3 The singular integral equation

To derive the integral equations for the crack problem, the distributed dislocation technique is employed. The distributed dislocation technique is an efficient means to carry out the task, see for instance [18].

Let screw dislocation with density b_z is distributed on a moving crack in a functionally graded orthotropic strip. The stress fields caused by the above mentioned distribution of dislocation become

$$\sigma_{zy}(x,y) = b_z \times \begin{cases} k_{zy}^1(x,y,0,h_1), & 0 \le y \le h_1 \\ k_{zy}^2(x,y,0,h_1), & h_1 \le y \le h \end{cases} \tag{15}$$

Where $k_{zy}^l(x,y,0,h_1), \quad l=1,2$ are the coefficients of b_z and may be deduced from (13) and (14) for the two different formulations. The moving cracks configuration may be described in parametric form as

$$\begin{aligned} x_i &= x_{0i} + l_i s \\ y_i &= y_{0i} \qquad i = 1,2,...,N \qquad -1 \le s \le 1 \end{aligned} \tag{16}$$

We consider local coordinate systems moving on the face of i-th crack. The anti-plane traction on the face of the i-th crack in terms of stress components in Cartesian coordinates becomes:

$$\sigma_{nz}(x_i, y_i) = \tau_0 \tag{17}$$

Suppose dislocations with unknown density $B_{zj}(p)$ is distributed on the infinitesimal segment dl_j located at the face of the j-th crack where the parameter $-1 \le p \le 1$ and prime denotes differentiation with respect to the relevant argument. The traction on the face of i-th crack due to the presence of distribution of dislocations on the face of all N cracks yields

$$\sigma_{nz}(x_i(s), y_i(s)) = \sum_{j=1}^{N} \int_{-1}^{1} k_{ij}(s,p) l_j B_{zj}(p) dp \qquad i = 1,2,...,N, \tag{18}$$

The kernel of integral (18) becomes:

$$k_{ij}(s,p)=\begin{cases}k_{zy}^{1}(x_i,y_i,x_j,y_j), & 0\le y_i\le y_j\\ k_{zy}^{2}(x_i,y_i,x_j,y_j), & y_j\le y_i\le h\end{cases} \tag{19}$$

The function $k_{zy}^{l}(x_i,y_i,x_j,y_j),\ l=1,2$ are introduced in (15), we should point out that in (19) quantities with subscript i are functions of s whereas those with subscript j are functions of p. The crack problem has been treated by means of the super position technique. By virtue of the Buckner's principal [19], the elasticity problem of a strip without any cracks has been solved and equal and opposite values of the stresses have been used as the traction on the cracks surfaces. Therefore, the left-hand side of Eq. (18) may be specified. In order to determine the singular behavior of Eq. (18), the behavior of kernel needs to be examined. For this, it is sufficient that r goes to zero, Where $r=\sqrt{(x_i(s)-x_j(p))^2+(y_i(s)-y_j(p))^2}$. Consequently, Eq. (18) is Cauchy singular integral equations for the dislocation densities.

Where from Eqs. (14), the kernel of integral equation is

$$\begin{aligned}k_{ij}(x_i(s),y_i(s),x_j(p),y_j(p))=&-\frac{\operatorname{sgn}(x_i(s)-x_j(p))\mu_{0y}e^{\lambda(y_i(s)+y_j(p))}}{2h}\\ &\times\sum_{n=1}^{\infty}[\cos(\frac{n\pi}{h}(y_j(p)-y_i(s)))-\cos(\frac{n\pi}{h}(y_j(p)+y_i(s)))]\\ &\times e^{\frac{-|x_i(s)-x_j(p)|}{f\sqrt{(1-V^2/C_x{}^2)}}\sqrt{(\frac{n\pi}{h})^2+\lambda^2}}\end{aligned} \tag{20}$$

We

Substitute Eq. (17) and (20) into Eq. (18), we obtain the following singular integral equations:

$$\begin{aligned}\sum_{j=1}^{N}\int_{-1}^{1}\{&-\frac{\operatorname{sgn}(x_i(s)-x_j(p))\mu_{0y}e^{\lambda(y_i(s)+y_j(p))}}{2h}\\ &\times\sum_{n=1}^{\infty}[\cos(\frac{n\pi}{h}(y_j(p)-y_i(s)))-\cos(\frac{n\pi}{h}(y_j(p)+y_i(s)))]\\ &\times e^{\frac{-|x_i(s)-x_j(p)|}{f\sqrt{(1-V^2/C_x{}^2)}}\sqrt{(\frac{n\pi}{h})^2+\lambda^2}}\}B_{zj}(p)l_j dp=\tau_0\end{aligned} \tag{21}$$

It is worth mentioning that kernels in integral Eq. (21) are Cauchy singular integral equations. Employing the definition of the dislocation density function, the equation for the crack opening displacement across the j-th crack becomes

$$w_j^{-}(s)-w_j^{+}(s)=\int_{-1}^{s}l_j B_{zj}(p)dp \qquad j=1,2,3,...,N, \tag{22}$$

The displacement field is single-valued for the faces of cracks. Consequently, the dislocation density functions are subjected to the following closure requirements

$$l_j\int_{-1}^{1}B_{zj}(p)dp=0, \qquad j=1,2,3,...,N \tag{23}$$

The Cauchy singular integral Equations (21) and (23) are solved simultaneously. To determine dislocation density functions this task is taken up by the methodology developed by Erdogan et al. [20]. The stress fields in the neighborhood of crack tips behave like $1/\sqrt{r}$ where r is the distance from the crack tip. Therefore, the dislocation densities are taken as

$$B_{zj}(p)=\frac{g_{zj}(p)}{\sqrt{1-p^2}}, \qquad -1\le p\le 1 \qquad j=1,2,3,...,N \tag{24}$$

Substituting Eq. (24) into Eqs. (18) and (23) and discretizating of the domain, $-1\le p\le 1$, by $m+1$ segments, we arrive at the following system of $N\times m$ algebraic equations

$$\begin{bmatrix} A_{11} & A_{12} & \cdots & A_{1N} \\ A_{21} & A_{22} & \cdots & A_{2N} \\ \vdots & \vdots & \ddots & \vdots \\ A_{N1} & A_{N2} & \cdots & A_{NN} \end{bmatrix}\begin{bmatrix} g_{z1}(p_n) \\ g_{z2}(p_n) \\ \vdots \\ g_{zN}(p_n) \end{bmatrix}=\begin{bmatrix} q_1(s_r) \\ q_2(s_r) \\ \vdots \\ q_N(s_r) \end{bmatrix}, \tag{25}$$

Where the collocation points are

$$\begin{cases} s_r=\cos(\dfrac{\pi r}{m}) & r=1,2,...,m-1 \\ p_n=\cos(\dfrac{\pi(2n-1)}{2m}) & n=1,2,...,m \end{cases} \tag{26}$$

The components of matrix in (25) are

$$A_{ij}=\frac{\pi}{m}\begin{bmatrix} k_{ij}(s_1,p_1) & k_{ij}(s_1,p_2) & \cdots & k_{ij}(s_1,p_m) \\ k_{ij}(s_2,p_1) & k_{ij}(s_2,p_2) & \cdots & k_{ij}(s_2,p_m) \\ \vdots & \vdots & \ddots & \vdots \\ k_{ij}(s_{m-1},p_1) & k_{ij}(s_{m-1},p_2) & \cdots & k_{ij}(s_{m-1},p_m) \\ \delta_{ij}l_i & \delta_{ij}l_i & \cdots & \delta_{ij}l_i \end{bmatrix}, \tag{27}$$

In (27), δ_{ij} in the last row of A_{ij} designates the Kronecker delta. The components of vectors in (25) are

$$\begin{aligned} &g_{zj}(p_n)=\left[g_{zj}(p_1) \quad g_{zj}(p_2) \quad \cdots \quad g_{zj}(p_m)\right]^T, \\ &q_j(s_r)=[\sigma_{yz}(x_j(s_1),y_j(s_1)) \quad \sigma_{yz}(x_j(s_2),y_j(s_2))... \quad \sigma_{yz}(x_j(s_{m-1}),y_j(s_{m-1})) \quad 0]^T, \end{aligned} \tag{28}$$

Where superscript T stands for the transpose of a vector. The stress intensity factors at the tip of i-th crack in terms of the crack opening displacement reduce to [21]

$$\begin{aligned} k_{Li}&=\frac{\sqrt{2}}{4}\mu(y_{Li})\lim_{r_{Li}\to 0}\frac{w_i^-(s)-w_i^+(s)}{\sqrt{r_{L_i}}}, \\ k_{Ri}&=\frac{\sqrt{2}}{4}\mu(y_{Ri})\lim_{r_{Ri}\to 0}\frac{w_i^-(s)-w_i^+(s)}{\sqrt{r_{R_i}}}, \end{aligned} \tag{29}$$

Where L and R designate, the left and right tips of a crack, respectively. The geometry of a crack implies:

$$\begin{aligned} r_{Li}&=\left[(x_i(s)-x_i(-1))^2+(y_i(s)-y_i(-1))^2\right]^{\frac{1}{2}}, \\ r_{Ri}&=\left[(x_i(s)-x_i(1))^2+(y_i(s)-y_i(1))^2\right]^{\frac{1}{2}}. \end{aligned} \tag{30}$$

In order to take the limits for $r_{Li}\to 0$ and $r_{Ri}\to 0$, we should let, in Eq. (31), the parameter $s\to -1$ and $s\to 1$, respectively. The substitution of (24) into (22), and the resultant equations and Eq. (30) into Eq. (29) in conjunction with the Taylor series expansion of functions $x_i(s)$ and $y_i(s)$ around the points $s\to\pm 1$ yields:

$$k_{Li} = \frac{\mu(y_{Li})f}{2}((x_i'(-1))^2 + (y_i'(-1))^2)^{\frac{1}{4}} g_i(-1),$$
$$k_{Ri} = -\frac{\mu(y_{Ri})f}{2}((x_i'(1))^2 + (y_i'(1))^2)^{\frac{1}{4}} g_i(1), \qquad i = 1,2,3,...,N. \tag{31}$$

The solutions of (27) are plugged into (31) thereby the stress intensity factors are obtained. As well known, the stress intensity factor alone is not sufficient to estimate the dynamic behavior of crack initiation of the material. Therefore, the energy density factor is employed combining with the stress intensity factor to evaluating the ability of the crack propagation. According to the theory of strain energy density criterion [22,23], the strain energy density factors S at the crack tip can be expressed as

$$S = a_{11}K_I^{\ 2} + 2a_{12}K_I K_{II} + a_{22}K_{II}^{\ 2} + a_{33}K_{III}^{\ 2} \tag{32}$$

Where the coefficients $a_{33} = 1/4\pi\mu$, with μ the shear modulus of elasticity. Since there exist only K_{III} in this study, crack front can be obtained by substituting the functions of the stress intensity factor K_{III} in to Eq. (32); we arrive at

$$S = (1/4\pi\mu)K^2{}_{III} \tag{33}$$

4 Numerical calculations and discussion

In this section, several cases were examined to illustrate the validity and accuracy of the proposed method. The analysis developed in the preceding sections allows the consideration of a functionally graded orthotropic strip with multiple moving cracks. The attention will be focused on the effect of the speed of crack propagating and the gradient of the material properties upon the dynamic fracture behavior of material. The applied load in all examples is the anti-plane shear traction on the top and bottom face of the strip.

The first example is the problem of a crack located at the point $(0, h/2)$ with different ratios of shear moduli. For the case $l/h = 0.25$, the effects of material properties on the stress intensity factors are studied. The crack is propagating parallel to the strip surfaces with constant velocity V at time $t = 0$, in the positive x–direction. It is observed that dynamic stress intensity factor is increased with the increasing of the speed of propagating crack V/C. The trend of variation remains the same by changing the FGM constant and ratios of shear moduli.

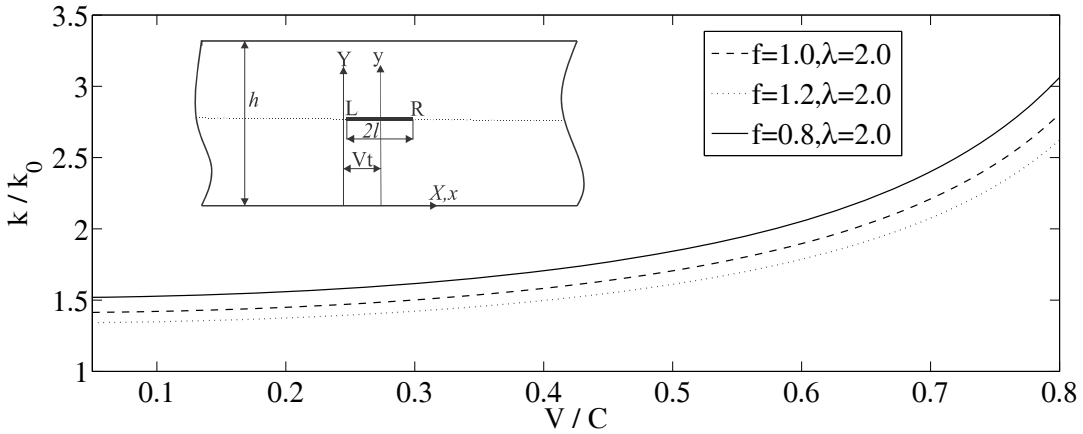

Figure 2 Variation of normalized stress intensity factor with crack propagation speed

Figure (3) shows the effects of gradient parameter λl, upon normalized stress intensity factor k/k_0, for a crack with different crack propagation speeds V/C. As it was expected, k/k_0 increases significantly with the increasing of the material parameter λl and k/k_0, increases with the increasing of V/C. It can be concluded that for functionally graded orthotropic strip parameter λl and the ratio of shear moduli have a great influence on the dynamic stress intensity factor.

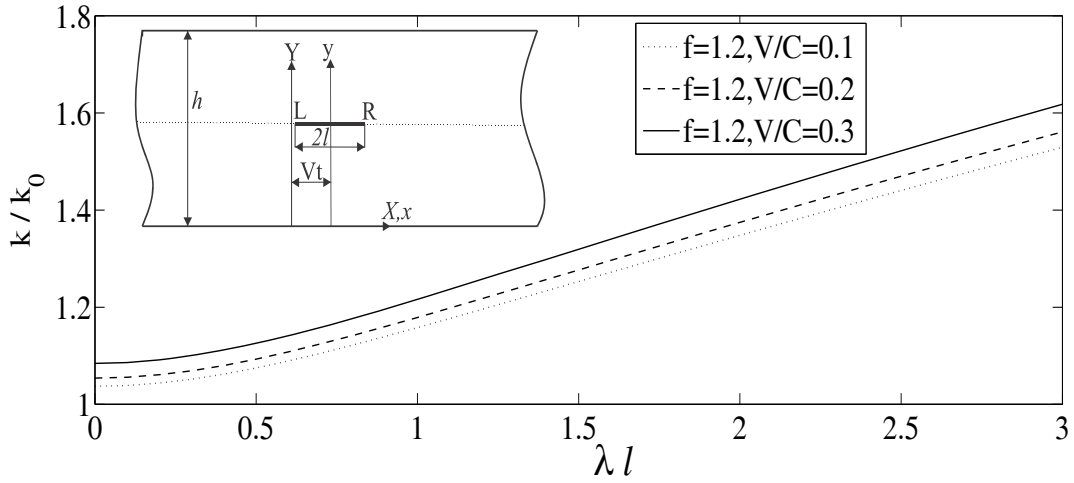

Figure 3 Variation of normalized stress intensity factor with gradient parameter λl

For studying the interactions between the multiple cracks, plots of stress intensity factors and strain energy density factors through figures (3-9) have been made. Consider the case where, the two collinear moving cracks with equal-length $2l$ are located on the center-line of the strip. Figure (4) shows the variation of the normalized dynamic stress intensity factor with the material parameter λl for the case Where $V/C = 0.8$. As it might be observed the maximum stress intensity factors for the crack tips R_1 and L_2 occur when the distance between them is minimal.

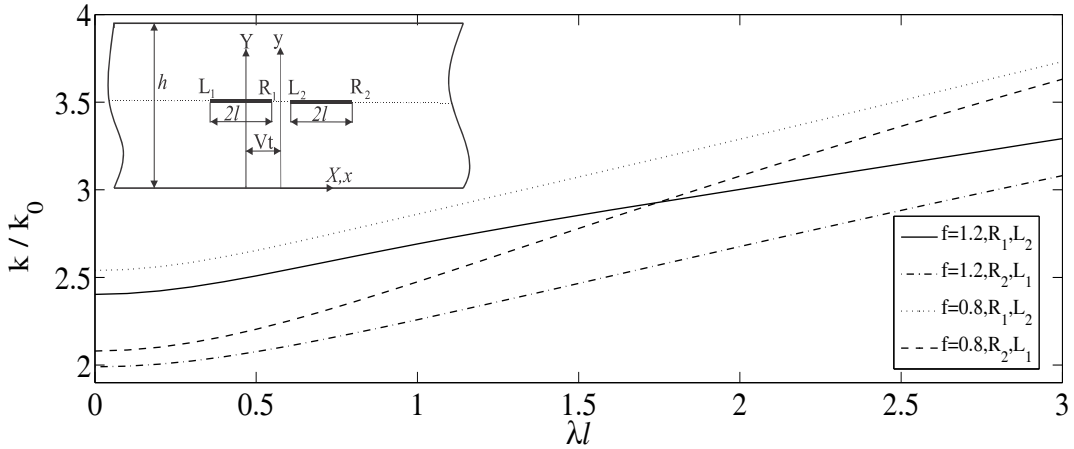

Figure 4 Variation of normalized stress intensity factor with gradient parameter for two collinear cracks

In the next work, we studied the variation of dimensionless SED, versus V/C with different FGM constants. Figure (5) shows the effect of the crack length upon the normalized strain energy density factor for FGM constant speed for the case where $f = 1.0$. The distance of the centers of cracks remains fixed while the cracks lengths are changing with the same rate. For

static problem, where $V/C = 0.0$, changing the crack length shows the weakest effect on k/k_0. Here, the dynamic stress intensity factors for both adjacent tips are increased with crack length.

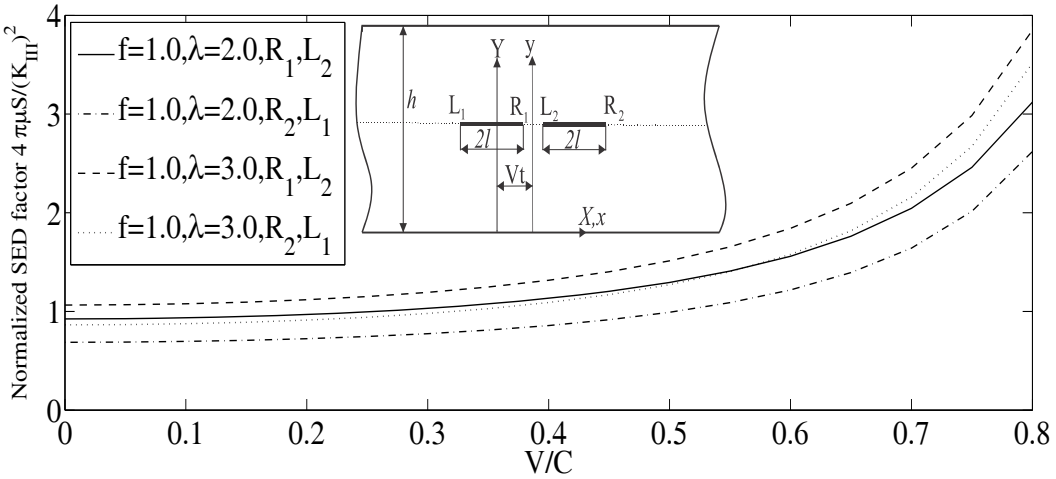

Figure 5 Variation of strain energy density factors with crack propagation speed

Figure (6) displayed, the variation of normalized stress intensity factors with the crack length for the case of $V/C = 0.0$ and $V/C = 0.8$. Note that as the velocity of the cracks increase, the amplitudes of the normalized stress intensity factors increase with a faster rate. For other values of material parameter same trend of variation of k/k_0 with different values may be obtained.

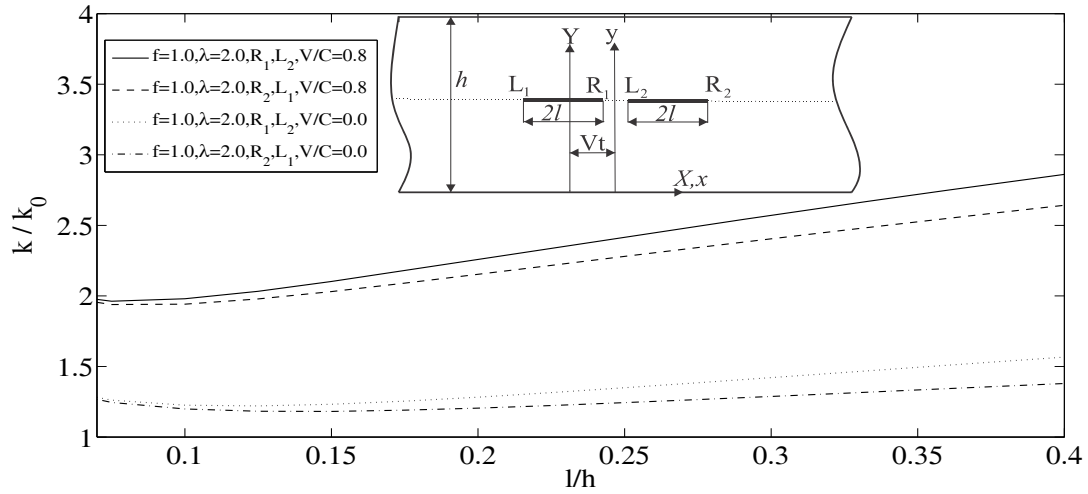

Figure 6 Variation of stress intensity factor of two collinear cracks versus l/h.

In the next example, we studied the dynamical behavior of functionally graded orthotropic strip with parallel cracks which figure (7) and (8) displayed, respectively, the variation of the normalized stress intensity factors versus material parameter λl and l/h for the case of $f = 1.2$. Figure (7) shows the effects of gradient parameter λl upon normalized stress intensity factor. It is observed that k/k_0 increases with increasing of the material parameter.

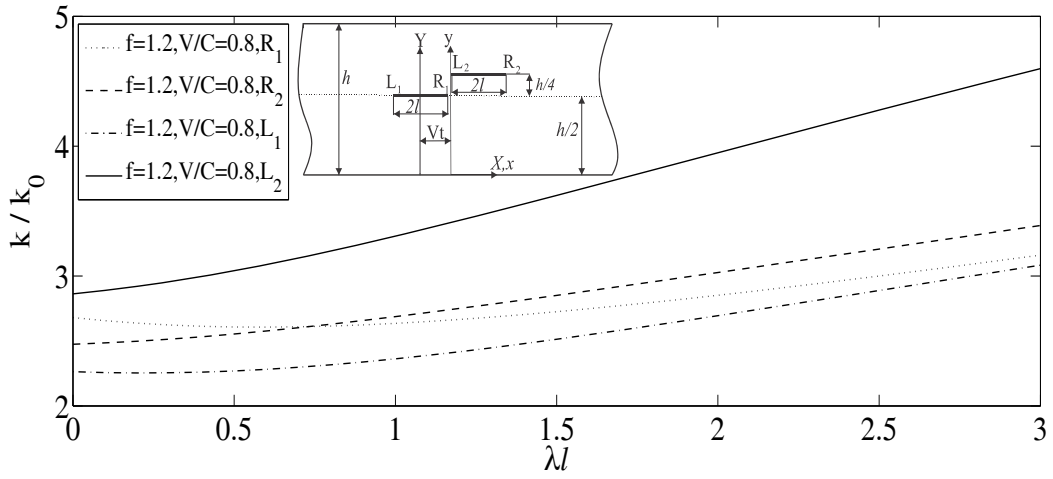

Figure 7 Variation of stress intensity factor of two parallel cracks with gradient parameter λl

Figure (8) shows the effect of the crack length upon the normalized stress intensity factor for the case where $V/C = 0.8$. Here, the dynamic stress intensity factor increases with increasing of l/h.

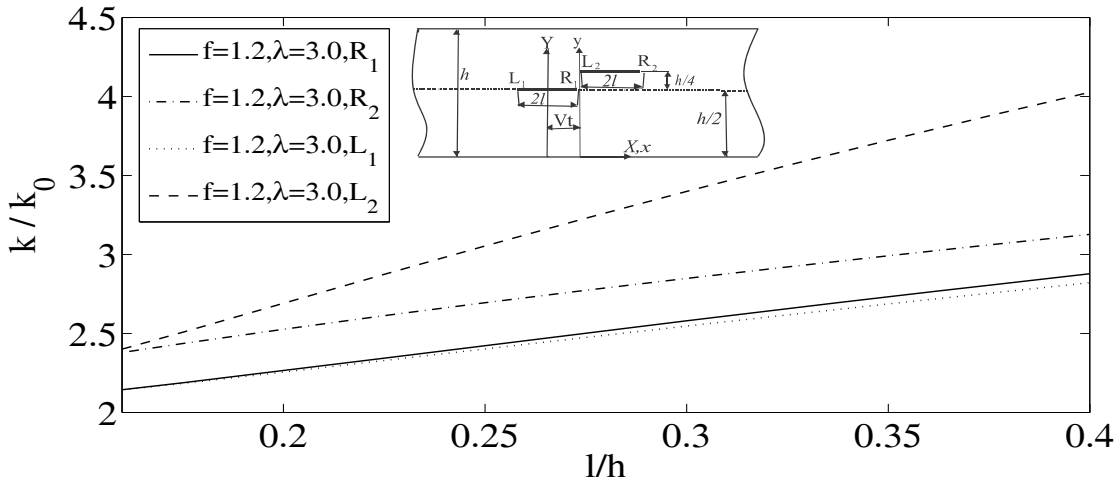

Figure 8 Variation of stress intensity factor of two parallel cracks with l/h.

Numerical results of strain energy density for two parallel cracks as a function of the crack speed ratio V/C for $f = 1.0$ and $\lambda = 2.0$ are depicted in figure (9). It is seen that SEDs increases as V/C is increased.

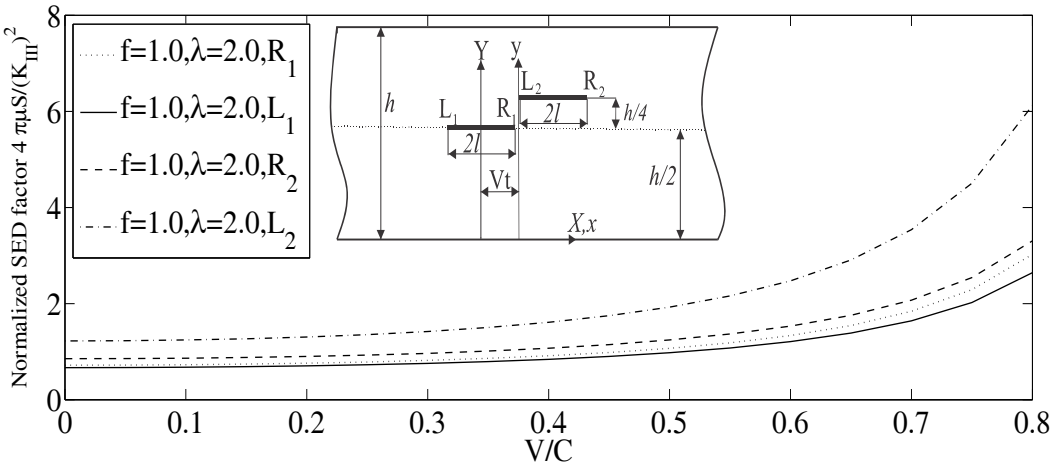

Figure 9 Variation of strain energy density factor of two parallel cracks versus V/C .

5 Conclusions

In this study, we have developed on the stress analysis of a functionally graded orthotropic strip weakened by screw dislocation. The stress components are used as the Green's function to derive integral equations for the analysis of multiple moving cracks. The dependence of the fracture behavior on the crack propagation velocity and gradient of the material properties was shown in the numerical results. Reasonable agreement between the present study and the other solutions were obtained. To show the applicability of the procedure more examples are solved where in the interaction between cracks is investigated.

References

[1] Freund, L.B., "*Dynamic Fracture Mechanics*", Cambridge University Press, (1998).

[2] Yoffe, E.H., "The Moving Griffith Crack", Philosophical Magazine, Vol. 42, pp. 739-750, (1951).

[3] Sih, G.C., and Chen, E.P., "Moving Cracks in Layered Composites", International Journal of Engineering Science, Vol. 20, pp. 1181–1192, (1982).

[4] Wang, X.D. and Meguid, S. A., "On the Dynamic Crack Propagation in an Interface with Spatially Varying Elastic Properties", International Journal of Fracture, Vol. 69, pp. 87–99, (1994).

[5] Meguid, S.A., Wang, X.D., and Jiang, L.Y., "On the Dynamic Propagation of a Finite Crack in Functionally Graded Materials", Engineering Fracture Mechanics, Vol. 69, pp. 1753–1768, (2002).

[6] Jiang, L.Y., and Wang, X.D., "On the Dynamic Propagation in an Interphase with Spatially Varying Elastic Properties under In-plane Loading", International Journal of Fracture, Vol. 114, pp. 225–244, (2002).

[7] Bi, X.S., Cheng, J., and Chen, X.L., "Moving Crack for Functionally Grated Material in an Infinite Length Strip under Anti-plane Shear", Theoretical and Applied Fracture Mechanics, Vol. 39, pp. 89-97, (2003).

[8] Li, X.F., "Griffith Crack Moving in a Piezoelectric Strip", Archive of Applied Mechanics, Vol. 72, pp. 745-758, (2003).

[9] Kwon, S.M., "On the Dynamic Propagation of an Anti-plane Shear Crack in a Functionally Graded Piezoelectric Strip", Acta Mechanica, Vol. 167, pp. 73-89, (2004).

[10] Ma, L., Wu, L.Z., and Guo, L.C., "On the Moving Griffith Crack in a Non-homogeneous Orthotropic Strip", International Journal of Fracture, Vol. 136, pp. 187-205, (2005).

[11] Das, S., "Interaction of Moving Interface Collinear Griffith Cracks under Anti-plane Shear", International Journal of Solids and Structures, Vol. 43, pp. 7880-7890, (2006).

[12] Singh, B.M., Rokne, J., Vrbik, J., and Dhaliwal, R.S., "Finite Griffith Crack Propagating in a Non-homogeneous Medium", European Journal of Mechanics, A. Solids, Vol. 25, pp. 867-875, (2006).

[13] Wang, B.L. and Han, J.C., "A Moving Crack in a Non-homogeneous Material", Acta. Mechanica Solid Sinica, Vol. 19, pp. 223-230, (2006).

[14] Wang, B.L., and Han, J.C., "A Mode III Moving Crack between a Functionally Graded Coating and Homogeneous Substract", Journal of Mechanics of Materials and Structures, Vol. 1, pp. 649-661, (2006).

[15] Cheng, Z., and Zhong, Z., "Analysis of a Moving Crack in a Functionally Graded Strip between Two Homogeneous Layers", International Journal of Mechanical Sciences, Vol. 49, pp. 1038-1046, (2007).

[16] Bagheri, R., and Ayatollahi, M., "Multiple Moving Cracks in a Functionally Graded Strip", Applied Mathematical Modelling, Vol. 36, pp. 4677-4688, (2012).

[17] Weertman, J., and Weertman, J.R., "*Elementary Dislocation Theory*", Oxford University Press, New York, (1992).

[18] Weertman, J., "*Dislocation Based Fracture Mechanics*", World Scientific Publishing Co., Singapore, (1996).

[19] Hills, D.A., Kelly, P.A., Dai, D.N. and Korsunsky, A.M., "*Solution of Crack Problems: The Distributed Dislocation Technique*", Kluwer Academic Publishers, (1996).

[20] Erdogan, F., Gupta, G.D., and Cook, T.S., "*Numerical Solution of Singular Integral Equations Method of Analysis and Solution of Crack Problems*", Edited by G.C. Sih, Noordhoos, Leyden, Holland, (1973).

[21] Erdogan, F., "The Crack Problem for Bonded Non-homogeneous Materials under Anti-plane Shear Loading", Trans. ASME, J. Appl. Mech. Vol. 52, pp. 823–828, (1985).

[22] Sih, G.C., “A special Theory of Crack Propagation: Method of Analysis and Solutions of Crack Problems”, in: Sih(Ed.), G.C., *Mechanics of Fracture I*, Noordhoof International Publishing, Leyden, pp. 21-45, (1973),

[23] Sih, G.C., “A Three Dimensional Strain Energy Density Theory of Crack Propagation: Three Dimensional of Crack Problems”, in: Sih (Ed.), G.C., *Mechanics of Fracture II*, Noordhoof International Publishing, Leyden, pp. 15-53, (1975),

Nomenclature

l	half lengths of straight crack
A_{ij}	coefficients matrix
b_z	Burgers vector
B_{zj}	complex dislocation densities
C_x	shear wave velocity
$g_{zj}(p)$	regular terms of dislocation densities
$H(y)$	Heaviside step function
k_{Li}, k_{Ri}	stress intensity factors of left and right side of crack
k_0	stress intensity factor of a crack in infinite plane
$k_{ij}(s, p)$	kernel of integral equations
r_{Li}, r_{Ri}	distance from left and right crack tips
w	out of plane displacement component
x, y	coordinates
δ_{ij}	Kronecker delta
μ_{0x}, μ_{0y}	elastic shear modulus
ρ	mass density
σ_{nz}	traction vector
σ_{xz}, σ_{yz}	out of plane stress components

چکیده

از روش توزیع نابجایی برای تحلیل تنش در باریکه ساخته شده از مواد تابعی ارتوتروپیک حاوی چندین ترک متحرک تحت بارگذاری پاد صفحه ای استفاده شده است. ابتدا با استفاده از تبدیل فوریه میدان تنش در اثر نابجایی در باریکه بدست می آید، سپس با داشتن این حل، معادلات انتگرالی توزیع نابجایی روی ترک ها تعیین می شود. این معادلات دارای تکینگی از نوع کوشی هستند. حل معادلات تکین از نوع کوشی بصورت عددی انجام شده است. در پایان تعدادی مثال حل شده که در آنها اثر خواص ماده، طول ترک، هندسه محیط و نیز سرعت حرکت ترک بر روی ضرایب شدت تنش دینامیکی بررسی شده است.